Structural Analysis of Historical Constructions – Jerzy Jasieńko (ed)
© 2012 DWE, Wrocław, Poland, ISSN 0860-2395, ISBN 978-83-7125-216-7

QUANTITATIVE MONITORING OF SUPERFICIAL DECAY EVOLUTION IN PLASTERED AND UNPLASTERED OUTDOORS MASONRY

Bitelli Gabriele[1], *Colla Camilla*[2], *Gabrielli Elena*[3], *Girardi Fabrizio*[4], *Ubertini Francesco*[5]

In masonry materials, the superficial decay is a widespread problem, both when the masonry is unplastered and with plaster. Aggressive environmental agents such as moisture and salts trigger the damage by propagating through the material capillary pores. Although studies have been carried out on salt crystallization and their damaging effects, for the preservation of masonry buildings, due to their high number and to their cultural importance, it is required to better investigate the phenomena on real cases in their specific microclimatic. For these purposes, it would be important to have at disposal testing and monitoring tools capable of following the evolution of these processes since the beginning. Repeated visual inspections are commonly used to monitor the superficial decay but this is a subjective and qualitative technique. It would be important to apply image based diagnostic techniques capable of providing quantitative information. High-resolution laser scanning by triangulation technique of the masonry surface has the advantage of being contactless and rapid.
In an experimental set up in Bologna, Italy, large-size brick masonry walls were built, stored outdoors and exposed to weathering over 2 summers. In a 2-header brick wall, one main face is unplastered and one plastered. Before the start of the second ageing season, moisture and salt capillary rise was simulated by low-concentrated sodium chloride solution (0.1% -wt). The aim was to favour solution evaporation and salt crystallization and provoke material damage. 3D data acquisition by a triangulation laser scanning system was repeated at the end of both seasons and meshes derived from point clouds data compared.
The proposed procedure successfully extracted quantitative information about areas of material spalling and detachment even in the initial phases of decay.

Keywords: *Monitoring, Decay, Masonry, Laser scanner, Plaster*

1. INTRODUCTION AND RESEARCH REQUIREMENTS

The material decay caused by aggressive environmental agents is a widespread problem in masonry surfaces both when they are unplastered and with plaster. These degradation processes are mainly caused by water which may penetrates into the material pores in different ways such as by capillarity, percolation or vapour. The water is also responsible of the transport of dissolved salts (eventually present) which during brine evaporation may precipitate as crystals on the external material surfaces or beneath them. It is the increase in size of the salt crystals inside the pores to cause tensions eventually to overpass the material resistance threshold [1, 2]. This phenomena, although common in masonry materials is rather complex as the resulting damage is due to the interaction of salts with the specific environmental condition.
Several studies have been carried out on salt crystallization and their damaging effects in porous materials but they are mainly aimed at investigating the behaviour of single material units by means of laboratory analysis [3, 4]. In addition, open questions are still remaining i.e. about the correlation between results from accelerated aging test and the real natural damage in structures or about proper

[1] Prof., DICAM Dept., Engineering Faculty, University of Bologna, gabriele.bitelli@unibo.it
[2] Dr., CIRI-EC and DICAM Dept., Engineering Faculty, University of Bologna, camilla.colla@unibo.it
[3] Ph.D. student., DICAM Dept., Engineering Faculty, University of Bologna, elena.gabrielli4@unibo.it
[4] Dr., DICAM Dept., Engineering Faculty, University of Bologna, fabrizio.girardi@unibo.it
[5] Prof., DICAM Dept., Engineering Faculty, University of Bologna, francesco.ubertini@unibo.it

techniques to be used in masonry structures for successfully monitoring the time evolution of these environmental effects. Moreover, for the preservation of masonry buildings, due to their high number and to their cultural importance, it is required to better investigate these phenomena directly on real cases in their specific microclimatic environment. Repeated visual inspections are commonly used to monitor such superficial decay but this is a subjective and qualitative technique.
Thus, for these purposes, it would be important to have at disposal non-destructive testing and monitoring tools capable of quantitatively detecting and following the evolution of these processes since the beginning.
Among the available surface imaging methods, there is a wide range of tools able to create 3D models of the objects; these have been used in the last several years in various application fields (civil and mechanical engineering, cultural heritage, medicine, forensics, etc) by considering various range of object sizes at different scales [5]. Nonetheless, two basic approaches can be distinguished: image-based systems, where 3D models are generated using digital images, and range-based systems that use scanning systems with different technologies [6].
The acquisition of 3D models by means of laser scanners, thanks to the technical development in the last few years coupled with the decrease in the cost of scanning equipment, as well as the spreading use of hardware with high computational and graphic capability, have made this technique accessible to a much larger audience. In addition, as the technique is contactless, rapid and able to provide quantitative information, it may be used for monitoring the superficial environmental decay in outdoors masonry.

2. AIM OF THE WORK

The research work herein presented was aimed at finding proper methodologies for following the evolution of degradation processes connected to moisture and salt movements in masonry since their initial stage. With this purpose, a large brick masonry wall, with one main side unplastered and one plastered, subjected to natural weathering and brine damp rise was studied by means of an image based diagnostic technique: high-resolution laser scanning by triangulation technique. In this paper the methodology followed for the diagnosis was presented together with some preliminary results of this on-going experimental campaign in order to evaluate the reliability of the technique in monitoring quantitatively the superficial decay evolution in masonry surfaces.

3. EXPERIMENTAL WORK

3.1. Description of the specimen

A 2-header masonry wall (specimen PNDA) of nominal dimensions 130 × 25 × 130 cm^3 (b × s × h), made of solid brick units and natural hydraulic lime mortar joints, 1 cm thick, was considered. The specimen presents one main face unplastered (front side) and one plastered (rear side). The plaster layer, 1 cm thick, was made by using the same mortar mix of the vertical and horizontal masonry joints (Fig. 1). In addition, in the front side, some inclusions of different stones (limestone and sandstone) have been inserted at different heights in the wall.


a)

b)

c)

Fig. 1 Masonry wall PNDA with basins for brine, at the base: a) front side, b) right-hand side, c) rear side, plastered (3 May 2011)

The wall was exposed to natural weathering (in the microclimate of Bologna, Northern Italy) over 2 summers; further, before the start of the second ageing season, moisture and salt capillary rise from the wall base was simulated by low-concentrated sodium chloride solution (0.1% -wt). This natural ageing process provokes material damage by favouring solution evaporation and salt crystallization on the masonry surface or beneath it.

3.2. 3D laser scanner survey

In this experimental work, a triangulating desktop laser scanner has been used, which is proven to be a reliable technology for non-contact surface measurements. The technique is called triangulation because the laser spot, the camera and the laser emitter form a triangle, and exploiting the principle of the topographic forward intersection it is possible to determine the position of a point in the 3D space defined by the instrumental reference system (Fig. 2). The distance between the laser emitter and the camera sensor (representing one side of the triangle) is known by the constructor specification, and it is called "baseline" (b). The out-coming angle (α) of the laser beam is also known by a prior calibration of the rotating mirror. Then the laser beam undergoes a reflection on the targeted surface, and its footprint on the receiving sensor (usually a CCD or CMOS), makes it possible to calculate the angle (β). These three informations (α, β, b) combined with the trigonometric formulas (1), (2), fully determine the coordinates of the points cloud in which the surface can be discretized.
Following a process of triangulation, the points cloud can be converted into a mesh of triangles, which constitute the 3D surface of the object. If the device is able to capture also the color RGB information, it is possible to texturize the surface. One acquisition is generally not sufficient to recover the entire surface for objects greater than the instrument's field of view. For this reason, in order to describe the entire surface in the best way, additional scan positions from different points of view are adopted.

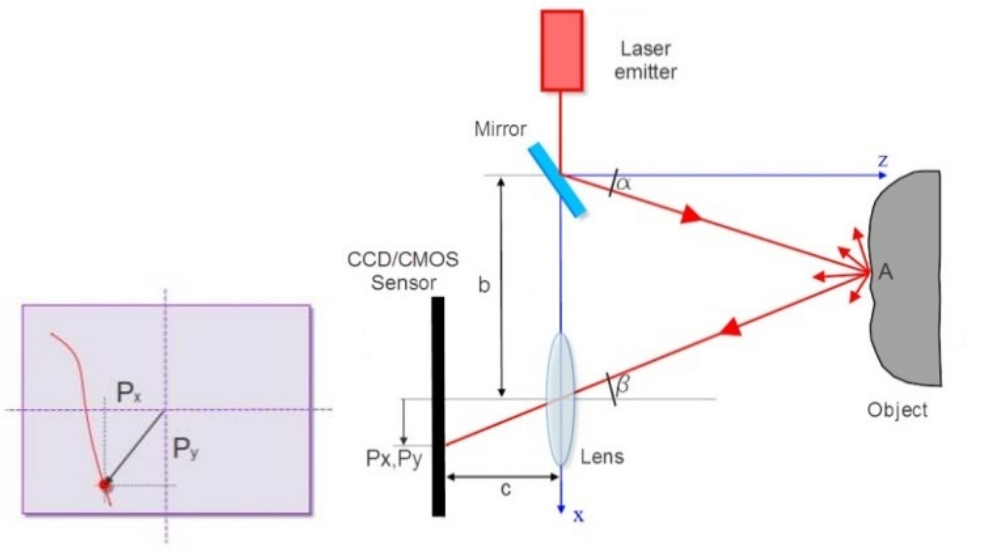

Fig. 2 Layout of a triangulation laser scanner

$$\tan\beta = \frac{P_x}{c} \quad ; \quad \tan\gamma = \frac{P_y}{c} \tag{1}$$

$$x_A = \frac{b}{1+\frac{\tan\beta}{\tan\alpha}} \quad ; \quad y_A = \frac{b}{\frac{\tan\alpha}{\tan\gamma}+\frac{\tan\beta}{\tan\gamma}} \quad ; \quad z_A = \frac{b}{\tan\alpha+\tan\beta} \tag{2}$$

3.3. Test equipments

The laser scanner used in this work is produced by NextEngine Inc. and is based on Multi-stripe Laser Triangulation (MLT) technology. The laser scanner acquires the data in two different modes corresponding to two different baselines: Macro mode and Wide mode. Some constraints on the distance between the object and the scanner are given for each mode (Table 1).

Table 1 NextEngine laser scanner specifications

Dimensions	224 × 91 × 277 mm	
	Macro Mode	**Wide Mode**
Field of View	13x10 cm	35x25 cm
Working distance	18 cm	40 cm
Accuracy	±127 µm	±381 µm
Resolution	200 DPI	75 DPI
Texture density	400 DPI	150 DPI
Points/sec	50000	50000

The choice of the scan mode depends on the object's size and the desired output accuracy. The scanner mounts a couple of twin arrays of Class four 1M 10-mW solid-state lasers with custom optics at a 650-nm wavelength. The scanner also features twin 3 MP CMOS RGB image sensors, and built-in white light texture illuminators [7, 8] This technique was chosen because it is contactless, rapid and capable of providing quantitative information, thus it could be helpful in order to monitor the degradation processes caused by moisture and salt movements since the beginning.

4. DATA ACQUISITION

The evolution of the superficial decay caused by aggressive environment on both main surfaces of wall PNDA was monitored by means of the above described laser scanner instrument.
The first acquisition campaign was carried out at the end of the 1st weathering season (October 2010) and the 2nd campaign was repeated after one year (November 2011) at the end of the 2nd ageing season.
Due to the small field of view of the instrument used, a single scan acquisition was not sufficient to capture the entire surface, although considering the "wide mode configuration" (25 × 35 cm) which is the more suitable field of view in this case, and a number of scan-positions was necessary for covering one stripe of the wall surface.
Thus, in both measurement campaigns, multiple scans have been recorded, overlapping a certain area between two contiguous scans, and then combining them together.
Despite this, due to the large dimensions of the wall compared with the instrument field of view, only two vertical sections of the specimen have been scanned (one on the front side and one on the rear side of the wall). This choice was made in order neither to not dilate excessively the data acquisition time nor the subsequent data analysis time. In detail, on the front side of the wall, the vertical section A-A was surveyed by 6 scan-positions while on the rear, plastered side, the central section (B-B) was considered by means of 8 scan-positions (Fig. 3).

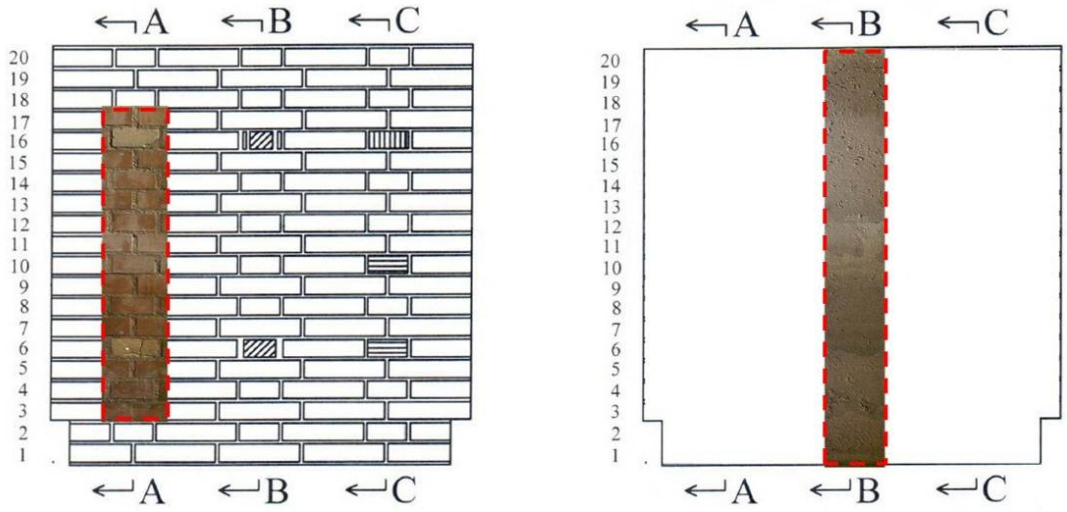

Fig. 3 Wall PNDA: monitored surfaces in the front-side (left) and back plastered side (right)

About one hour was required to scan each testing position. Note that every scanned area was recorded with its own particular reference system as it was not possible to establish and maintain in time a rigid reference system on the object framework due to logistical constraints of the laboratory setup (i.e. it was not feasible to cover the wall surfaces or a portion of them for a long period). All the measurements have been performed keeping the laser scanner perpendicular to the wall surface to be monitored, about 40 cm away from it and a tripod was used to vary the relative height of the instrument.
In this phase of the work, another problem encountered was the position of the brick wall because of its outdoors storage and of no protection against the sun. Critical environmental illumination, e.g. excessive brightness may badly affect the data acquisition as the used laser scanner is very sensitive to this parameter. This results in poor RGB colours, and in poor separation between the laser line and the background colour of the surface, hence making detection difficult. To avoid these problems, the survey is better performed during the night, or after darkening the work environment with panels or curtains. In this experimental case, the 2nd option was followed and the masonry wall and the equipment were covered with a large plastic sheet creating a dark testing area below (Fig. 4).

Fig. 4 Masonry wall and surrounding testing area covered with a plastic sheet (left), example of laser scanner survey (right)

5. DATA VISUALIZATION AND ANALYSIS

5.1. Visualization of the data

As already mentioned, multiple scans have been collected at each measurement position in order to capture at least a section of the masonry surface; then, to visualize and analyze the whole set of data collected in each position, the scan images have to be combined together. First of all, as each mesh is oriented with its own scanner reference system, a relative repositioning was performed, aimed at reconstructing the original object geometry and thus at visualizing correctly the data.
In the preliminary phase of this process, the approximate 3D rototranslation matrix has been calculated by measuring at least 3 tie-points in 2 contiguous scans which are manually selected. The procedure has then continued involving an algorithm able to minimize the difference between two clouds of points: the Iterative Closest Point (ICP). This algorithm is conceptually simple; it iteratively estimates the transformation parameters necessary to minimize the distance between the points of two raw scans and then it transforms the coordinates using such values. Thus, a fine alignment of each scan can be obtained. Once all the meshes are aligned in the same reference system, they have been merged together in order to create an only surface.
This process has been followed for each of the two measurement campaigns thus obtaining surfaces consisting of 3D merged models that can be compared between each other (Fig. 5, Fig. 6).

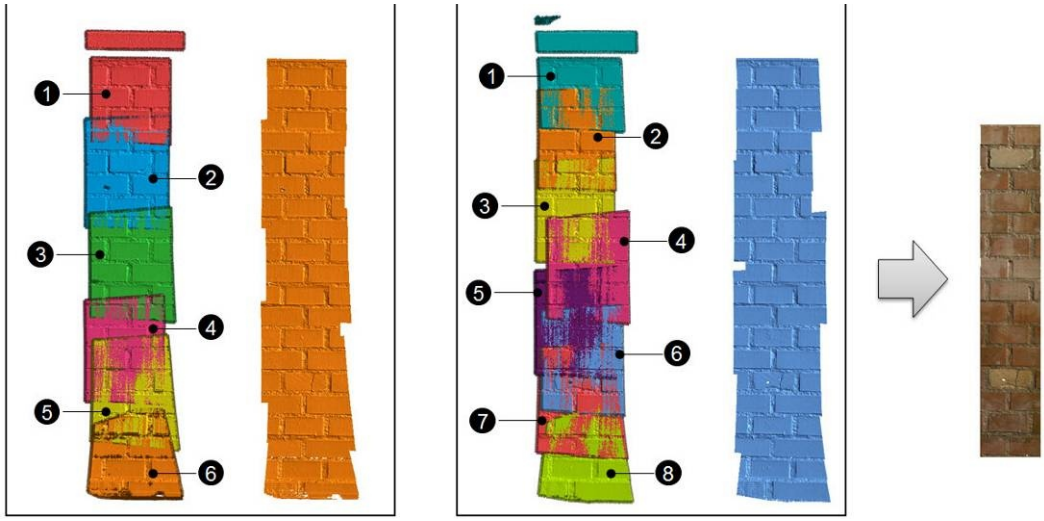

Fig. 5 PNDA Front, footprints of the scan-positions and 3D merged models of 2010 (left) and 2011 (center), texturized sub-area (right)

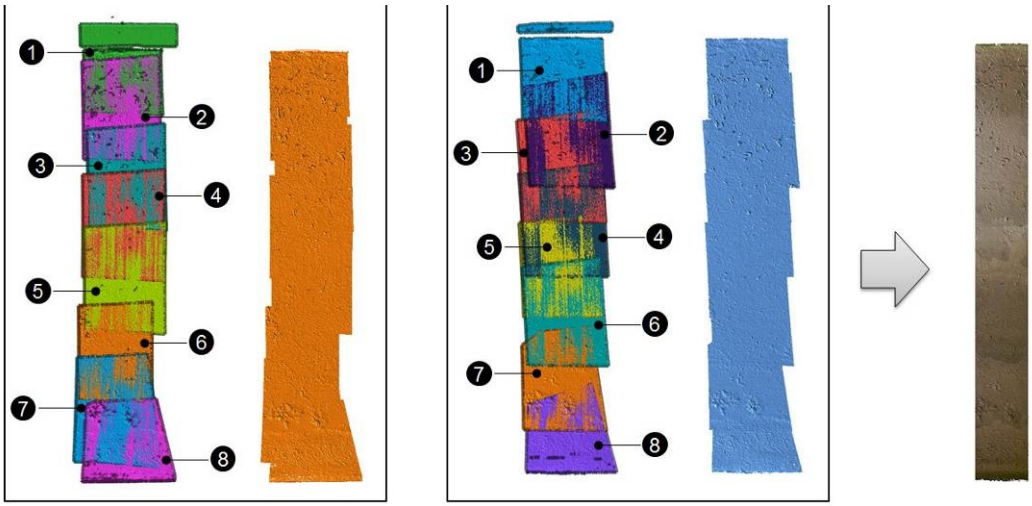

Fig. 6 PNDA Back: footprints of the scan-positions and 3D merged models of 2010 (left) and 2011 (center), texturized sub-area (right)

During this "merging" procedure, problems that may occur in this kind of test have been encountered. It is known, that with elongated and plane objects where the scans are essentially positioned along one direction, problems may arise with their alignment. If the central scans are strongly connected to each other, the scans at the extremes present only one side constrained and the residuals are usually larger in this area. This occurs in our case, and thus, not to affect the data quality a sub-area has been chosen for each monitored position.

5.2. Data analysis and discussion of results

The meshes derived from the point clouds measured at the end of each ageing period have been used separately, first of all, to perform a visual inspection. This is possible, with 3D model, especially when a photographic texture is superimposed to the mesh. In detail, some detachment areas and areas with material losses have been identified in both measuring campaigns. Thus, it was possible to detect the appearance of superficial decay also at the very beginning phases of natural weathering.

In order to make considerations over the variations over time in the 3D geometry of the object caused by material spalling, or to salt crystallization cycles, the surface "2010" was subtracted to the "2011" one, generating a displacement map. In Fig. 7, the 2011-2010 difference displacements maps for both sides of the wall are presented.

The highest and lowest values correspond to a major change of the surface occurred in time are reported in Fig. 7. In the front side, not plastered, the greater area of negative displacements is visible at masonry course 6 (from the base) in the natural stone inclusion. Thus, it seems that this material was more sensitive to the natural environmental ageing than the bricks or the mortar layers.

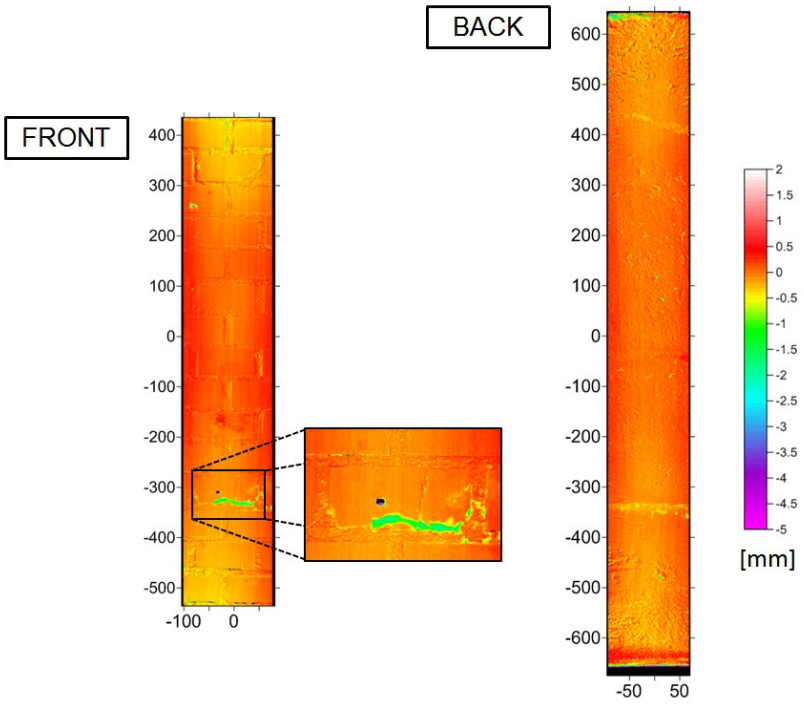

Fig. 7 Displacement map in [mm]: PND-A Front and Back

In the rear side, the greater negative displacements are concentrated along a straight horizontal line that is located at about the same height from the wall base that in the front side, which approximately corresponds to the level of moisture rise. In addition, some sparse pitting phenomena can be identified in the entire plastered surface.

For a more thorough study of the surface it is possible to split the changes affecting each constituent material. Thus, in this case two classes have been created: one concerning the bricks and one for the mortar layers, considering the stones as part of the "brick" class. In addition, it has been created a third class concerning the outliers: outliers are errors that have been easily recognized by the operator. In detail, in this specific case some displacements were caused by the presence of labels sparse in the surface. These labels were present only in one of the two years, and their presence, when the surface comparison is performed, could be incorrectly interpreted as a material variation.

By examining the three classes, called respectively Bricks, Mortar and Outliers, the percentage of material that can be considered acquired (positive values) or lost (negative values) are represented with cake diagrams (Fig. 8). The material belongs to one class instead of the other according to the threshold used. The threshold value correspond to the instrumental accuracy in the Wide mode ($\sigma = \pm$ 0.381 mm). Thus, the areas with displacements contained in this range can be considered without surface variations.

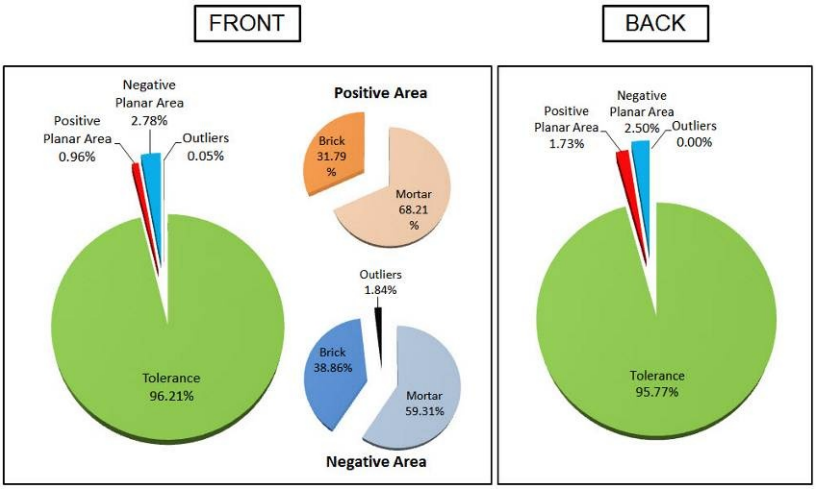

Fig. 8 PND-A diagrams

Table 2 Analysis of the comparison between the 2011 and 2010 3D model

PND-A Front	Class	Positive Z > +0.381	Negative Z < −0.381	In tolerance
Area (mm^2)	Mortar	1115.97	2819.30	
	Brick	520.13	1847.07	
	Outliers	0.00	87.26	
	Tot	1636.10	4753.63	164381.35
Volume (mm^3)	Mortar	113.60	463.71	
	Brick	41.48	609.40	
	Tot	155.08	1073.12	
PND-A Back		Positive Z > +0.381	Negative Z < −0.381	In tolerance
Area (mm^2)	Tot	3603.04	5221.12	199848.47
Volume (mm^3)	Tot	834.65	3105.20	

From these data, it is possible to note that both surfaces of the wall have suffered some damages, despite of the different orientation and the presence of plaster. In both surfaces, the negative areas are almost two times greater than the positive, acquired areas (in percentage). However, the rear side, although it is exposed to the North, presents more changes than the surface without plaster.
In the latter, it seems that the moisture and salt movements have affected greater the mortar than the brick surfaces. The decay of the mortar appears almost in the same percentage as swelling or salt crystallizations (positive areas) and material losses (negative areas). In the bricks, the negative areas are also due to material losses; instead, the positive areas are only apparent because the volume increase is mainly due to some flakes that are separating at this time point (material losses).

6. CONCLUSION

In an experimental set up in Bologna, Italy, a 2-header brick wall with one main face unplastered and one plastered has been considered. This masonry specimen has been subjected to moisture and low-concentrated sodium chloride solution (0.1% -wt) rise from the base.
The resulting superficial decay has been monitored by means of a 3D tool. In particular, laser data acquisitions were performed on selected area of the wall and repeated at the end of two ageing seasons. Multiple scans have been recorded and then combined together. In order to make considerations among the variations over time in the 3D geometry of the object caused by material spalling that are coming out, or to some salt crystallization cycles, the surface collected in “2010” was subtracted to the “2011” ones, generating a difference displacements map. In addition, the changes affecting the surfaces have been split among the construction materials (bricks and mortar) and the percentage of material that can be considered acquired (positive values) or lost (negative values) are represented with cake diagrams.
From this preliminary result it is possible to conclude that the proposed procedure was able to successfully extract quantitative information about areas of material spelling and detachment in unplastered and plastered masonry even in the initial phases of decay.

ACKNOWLEDGEMENTS

The authors would like to thank the European Commission for founding the FP7-ENV-2007-1 SMooHS – Project-Number: 212939 (*www.smoohs.eu*) and the project officer M. Chapuis.

REFERENCES

[1] Binda L., Baronio G. (1987) Mechanisms of Masonry Decay Due to Salt Crystallization. *Durability of Building Materials*, n.4, Elsevier, Amsterdam, 227-240.

[2] Scherer G.W. (2004) Stress from crystallization of salt. *Cement and Concrete Research,* 34: 1613-1624.
[3] Wendler E. (2002) Laboratory measurement on salt-loaded brick samples in periodically changing climate conditions. *The study of Salt Deterioration Mechanisms*, Ed. T. von Konow, Helsinki, Finland, 81-87.
[4] Lubelli B. (2006) *Sodium chloride damage to porous building materials*. PhD Thesis.
[5] Blais, F. (2004) A review of 20 years of range sensors development. *J. Electronic Imaging*, 13: 231-240.
[6] Sansoni G.; Trebeschi M.; Docchio F. (2009) State-of-The-Art and Applications of 3D Imaging Sensors in Industry, Cultural Heritage, Medicine and Criminal Investigation. *Sensors*, 9: 568-601.
[7] Bitelli G., Simone A., Girardi F., Lantieri C. (2009) Caratterizzazione di superficie e tessitura del manto stradale mediante tecniche a scansione laser, *Bollettino SIFET*, 3: 55-68.
[8] Guidi, G.; Remondino, F.; Morlando, G.; Del Mastio, A.; Uccheddu, F.; Pelagotti, A. (2007) Performances evaluation of a low cost active sensor for cultural heritage documentation, In: *8th Optical 3D*, Zurich, 9-12 July, 59-69.